Modulation of ACD6 dependent hyperimmunity by natural alleles of an Arabidopsis thaliana NLR resistance gene — Source link

Wangsheng Zhu, Maricris Zaidem, Anna-Lena Van de Weyer, Rafal M. Gutaker ...+9 more authors

Institutions: Max Planck Society

Related papers:

- Activation of the Arabidopsis thaliana Immune System by Combinations of Common ACD6 Alleles

- Autoimmune response as a mechanism for a Dobzhansky-Muller-type incompatibility syndrome in plants.

- Natural selection for polymorphism in the disease resistance gene Rps2 of Arabidopsis thaliana.

- Complex evolutionary events at a tandem cluster of Arabidopsis thaliana genes resulting in a single-locus genetic incompatibility.

- Genotype-Specific Expression and NLR Repertoire Contribute to Phenotypic Resistance Diversity in Plantago lanceolata.

Share this paper:

View more about this paper here: https://typeset.io/papers/modulation-of-acd6-dependent-hyperimmunity-by-natural-3vpmw0zgxe

RESEARCH ARTICLE

Modulation of *ACD6* dependent hyperimmunity by natural alleles of an *Arabidopsis thaliana* NLR resistance gene

Wangsheng Zhu[1☯], Maricris Zaidem[1☯¤a], Anna-Lena Van de Weyer[1], Rafal M. Gutaker[2¤a], Eunyoung Chae[1¤b], Sang-Tae Kim[1¤c], Felix Bemm[1], Lei Li[1], Marco Todesco[1¤d], Rebecca Schwab[1], Frederik Unger[1], Marcel Janis Beha[1], Monika Demar[1], Detlef Weigel[1]*

1 Department of Molecular Biology, Max Planck Institute for Developmental Biology, Tübingen, Germany, 2 Research Group for Ancient Genomics and Evolution, Max Planck Institute for Developmental Biology, Tübingen, Germany

☯ These authors contributed equally to this work.
¤a Current address: Center for Genomics and Systems Biology, New York University, New York, New York, United States of America
¤b Current address: Department of Biological Sciences, National University of Singapore, Singapore, Singapore
¤c Current address: Center for Genome Engineering, Institute for Basic Science, Yuseong-gu, Daejeon, South Korea
¤d Current address: Department of Botany, University of British Columbia, Vancouver, British Columbia, Canada
* weigel@weigelworld.org

🔓 OPEN ACCESS

Abstract

Plants defend themselves against pathogens by activating an array of immune responses. Unfortunately, immunity programs may also cause unintended collateral damage to the plant itself. The quantitative disease resistance gene *ACCELERATED CELL DEATH 6* (*ACD6*) serves to balance growth and pathogen resistance in natural populations of *Arabidopsis thaliana*. An autoimmune allele, *ACD6*-Est, which strongly reduces growth under specific laboratory conditions, is found in over 10% of wild strains. There is, however, extensive variation in the strength of the autoimmune phenotype expressed by strains with an *ACD6*-Est allele, indicative of genetic modifiers. Quantitative genetic analysis suggests that *ACD6* activity can be modulated in diverse ways, with different strains often carrying different large-effect modifiers. One modifier is *SUPPRESSOR OF NPR1-1, CONSTITUTIVE 1* (*SNC1*), located in a highly polymorphic cluster of nucleotide-binding domain and leucine-rich repeat (NLR) immune receptor genes, which are prototypes for qualitative disease resistance genes. Allelic variation at *SNC1* correlates with *ACD6*-Est activity in multiple accessions, and a common structural variant affecting the NL linker sequence can explain differences in SNC1 activity. Taken together, we find that an NLR gene can mask the activity of an *ACD6* autoimmune allele in natural *A. thaliana* populations, thereby linking different arms of the plant immune system.

Author summary

Plants defend themselves against pathogens by activating immune responses. Unfortunately, these can cause unintended collateral damage to the plant itself. Nevertheless, some wild plants have genetic variants that confer a low threshold for the activation of immunity. While these enable a plant to respond particularly quickly to pathogen attack, such variants might be potentially dangerous. We are investigating one such variant of the immune gene *ACCELERATED CELL DEATH 6* (*ACD6*) in the plant *Arabidopsis thaliana*. We discovered that there are variants at other genetic loci that can mask the effects of an overly active *ACD6* gene. One of these genes, *SUPPRESSOR OF NPR1-1, CONSTITUTIVE 1* (*SNC1*), codes for a known immune receptor. The *SNC1* variant that attenuates *ACD6* activity is rather common in *A. thaliana* populations, suggesting that new combinations of the hyperactive *ACD6* variant and this antagonistic *SNC1* variant will often arise by natural crosses. Similarly, because the two genes are unlinked, outcrossing will often lead to the hyperactive *ACD6* variants being unmasked again. We propose that allelic diversity at *SNC1* contributes to the maintenance of the hyperactive *ACD6* variant in natural *A. thaliana* populations.

Introduction

Plants rely on a sophisticated immune system to defend themselves against pathogens. A central challenge for plants is how to achieve a fast, effective response upon pathogen attack, while at the same time preventing spontaneous firing of the signaling machinery in the absence of danger [1]. Inappropriate activation of immune signaling can reduce growth or even damage the plant's own cells, while an inefficient immune response makes plants more likely to succumb to pathogen attack [2–6]. Although highly effective immune alleles may have background activity, they will nevertheless be favored when pathogen pressure is high. In contrast, in locations and years with low pathogen pressure, such alleles tend to be selected against [7]. If differently active alleles exist at the same locus, such temporal or spatial variation in pathogen pressure will maintain both types of alleles at ratios that reflect the prevalence of the different environments; this is one example of the phenomenon of balancing selection [8–10]. Very different alleles have been described for several disease resistance (R) genes of the nucleotide binding site leucine-rich repeat (NLR) class, although formal evidence for balancing selection is still rare [11–15]. NLR immune receptors detect the presence of so-called pathogen effector molecules, leading to effector-triggered immunity (ETI). NLRs do so in several different ways, and the biochemical and structural basis for effector detection, including direct interaction with effectors or with effector-modified host proteins, is increasingly well understood [16,17]. Variation in NLR immune receptors is linked to the fact that effectors are rarely essential for pathogen survival, and that even closely related pathogens can greatly vary in effector content [16,18].

In mutant screens, gain-of-function alleles have been identified for several NLR genes, based on their autoimmune phenotypes. The mutant proteins are active regardless of effector presence, and thus can increase resistance to a range of unrelated pathogens [19–26]. Whether highly active autoimmune alleles of NLR genes are being deployed to enhance broad-spectrum pathogen resistance in nature is unknown, but the presence of NLR alleles with modest autoimmune activity in breeding programs is well documented, and phenotypic signs of autoimmunity have been exploited to follow resistance genes in segregating crop populations (e.g., [27]).

In addition to specialized NLRs, which often engender very strong, qualitative disease resistance, plants employ various genes for quantitative resistance [28–31]. An example in the wild plant *A. thaliana* is *ACCELERATED CELL DEATH 6* (*ACD6*) [32–35]. Although *ACD6* does not encode an NLR immune receptor, the locus features extensive copy number and sequence variation in wild populations, reminiscent of what is found at many NLR loci. Importantly, natural populations segregate for *ACD6* allele classes with clear functional differences [36–38]. One class, first identified by genetic analysis of the natural Est-1 accession, protects in the greenhouse against a wide range of unrelated pathogens, from microbes to insects [36]. This unusually large benefit of the hyperactive *ACD6* allele appears to be due to enhanced and partially constitutive defense responses. On the other hand, the autoimmunity seen in plants with the *ACD6*-Est allele substantially compromises growth under specific laboratory conditions, reducing both plant size and the tempo with which new leaves are being produced [36,39,40]. That the allele is found at a frequency of over 10% in natural populations is compatible with the idea that selection maintains this allele despite a fitness trade-off [36–38]. The frequency of functionally distinct *ACD6* alleles differs between local populations, suggestive of a role of *ACD6* in local adaptation [37,38]. Alternatively, since the expression of immune and growth traits often differ between laboratory and field conditions [41–43], the effects the *ACD6*-Est allele in nature might be modified by the environment, and there is evidence from other laboratories that the expression of *ACD6*-Est associated lesions is environment-dependent [39,40,44,45].

ACD6 encodes a transmembrane protein with intracellular ankyrin repeats, which positively regulates cell death and defense, acting in part via the immune hormone salicylic acid (SA) and the SA transducer *NONEXPRESSER OF PR GENES 1* (*NPR1*) [32,33]. The precise mechanism of ACD6 biochemical action remains enigmatic, but ACD6 is found in a complex with several immune-related proteins, including pathogen-associated-molecular-pattern (PAMP) receptors, indicating a role for ACD6 in PAMP triggered immunity (PTI) [34,35]. While PTI and ETI have often been considered as different arms of the plant immune system, the distinction between ETI and PTI is becoming more and more blurred, not only because of substantial overlap in downstream responses, but also because not all effectors are highly variable, and not all PAMPs are highly conserved [46].

Here, we report that natural alleles at several independent loci can modulate the activity of the *ACD6*-Est autoimmune allele. We have characterized one locus, encoding the NLR protein SUPPRESSOR OF NPR1-1, CONSTITUTIVE 1 (SNC1) in detail and show that a common structural variant affecting the NL linker explains differences in *ACD6*-Est dependent SNC1 activity. We propose that allelic diversity at *SNC1* and other loci contributes to the maintenance of the *ACD6*-Est autoimmune allele in natural *A. thaliana* populations.

Results

Incidence of the *ACD6*-Est autoimmune allele in natural *A. thaliana* populations

Sanger sequencing analysis of a limited collection of 96 natural accessions had shown that 19, or 20%, had the *ACD6*-Est allele, which triggers autoimmunity and reduced growth under specific laboratory conditions [36]. To extend our knowledge of the global distribution of the *ACD6*-Est allele, we attempted to use Illumina short read data of 1,135 accessions [47,48], with the goal of ascertaining the presence of two codons that are causal for *ACD6*-Est autoimmune activity [36]. Likely because of linked sequence diversity and copy number variation, the first codon, encoding amino acid 566 in the reference sequence, GCA (Ala) in Col-0 and AAC (Asn) in Est-1, could not be confidently typed with short reads. At the second codon, encoding

amino acid 634 in the reference, 823 accessions could be assigned to have either Col-0- or Est-1-like codons. Of these, 721, or 88%, had CTT (Leu), diagnostic for the Col-0 reference, and 102, or 12%, had TTT (Phe), diagnostic for Est-1, confirming that *ACD6*-Est alleles are not uncommon in the global *A. thaliana* population.

Of the 19 accessions with an *ACD6*-Est allele examined by Todesco and colleagues [36], two did not show any necrotic lesions, an obvious sign of autoimmunity. The remaining 17 accessions differed in their phenotypic severity as well, with three classified as expressing mild, five intermediate, and nine strong necrosis. We extended this analysis to a total of 54 accessions for which we had confirmed the presence of an *ACD6*-Est allele by Sanger sequencing (S1 Table). Seven had no or only very mild lesions, 22 had intermediate lesions, and 25 were similarly affected as the Est-1 strain, in which this allele had been originally identified (Fig 1A).

Evidence for extragenic suppression of *ACD6*-Est alleles

While we could confirm that there is substantial variation in the extent of autoimmune phenotypes exhibited by *ACD6*-Est carriers, this observation did not inform about the genetic cause of this variation. To determine whether this was due to sequence differences at the *ACD6* locus itself, we directly tested *ACD6* activity in the first two *ACD6*-Est accessions identified as lacking necrotic lesions, Pro-0 and Rmx-A180 [36]. *ACD6* was expressed well in both accessions, indicating that suppression of the *ACD6*-Est phenotype was not due to reduced RNA accumulation (Fig 1B). We introduced full-length genomic *ACD6* fragments from both accessions into the Col-0 reference strain, which carries a standard *ACD6* allele, and into *acd6*-2, a Col-0 derivative with a T-DNA insertion in *ACD6*. All four classes of transformants from 10 T_1 lines had small rosettes and necrotic lesions, similar to what has been reported for Est-1 [36] (Fig 1C). Together, these results demonstrated that the *ACD6* alleles from Pro-0 and Rmx-A180 have similar activity as the original *ACD6*-Est allele outside their native genetic backgrounds, suggesting that accessions such as Pro-0 and Rmx-A-180 carry extragenic suppressors of *ACD6*-Est activity.

ACD6 acts in a feed-forward loop that regulates the accumulation of SA, a key hormone in both disease signaling and autoimmunity [49]. We therefore asked whether the suppressed autoimmunity of the *ACD6*-Est allele in Pro-0 was accompanied by reduced SA levels. Indeed, Pro-0 had much less SA than the *ACD6*-Est reference strain Est-1 or *acd6*-1, which carries an EMS-induced hyperactive *ACD6* allele in the Col-0 background [33]. SA levels in Pro-0 were even lower than in Col-0, which carries the standard *ACD6* allele (Fig 2A). Similarly, the expression of SA responsive marker gene *PR1* was reduced in Pro-0 compared to Est-1 (Fig 2B). As expected, knocking down *ACD6* with an artificial miRNA [36,50] resulted in greatly reduced SA levels in both *acd6*-1 and Est-1, while the effect in Pro-0 was much smaller (Fig 2A). In agreement, knocking-down *ACD6* in Pro-0 did not substantially affect *PR1* expression either (Fig 2B). Finally, to assess not only autoimmunity but also true immune responses, we measured H_2O_2 accumulation after stimulation with the PAMP flg22 [51]. Est-1 responded strongly to flg22, with the H_2O_2 production being greatly reduced by knocking down *ACD6*. Pro-0 responded much more weakly, and knocking down *ACD6* was of little consequence (Fig 2C). In conclusion, these results confirmed attenuation of the effects of the hyperactive *ACD6*-Est allele in Pro-0.

Modulation of *ACD6* hyperactivity by *RPP4/5* alleles

To understand the population genetic architecture underlying extragenic suppression of the activity of *ACD6*-Est-type alleles, we crossed three accessions that carried such alleles, but did not show necrosis, to the necrotic Est-1 accession. The ratios of necrotic and non-necrotic F_2
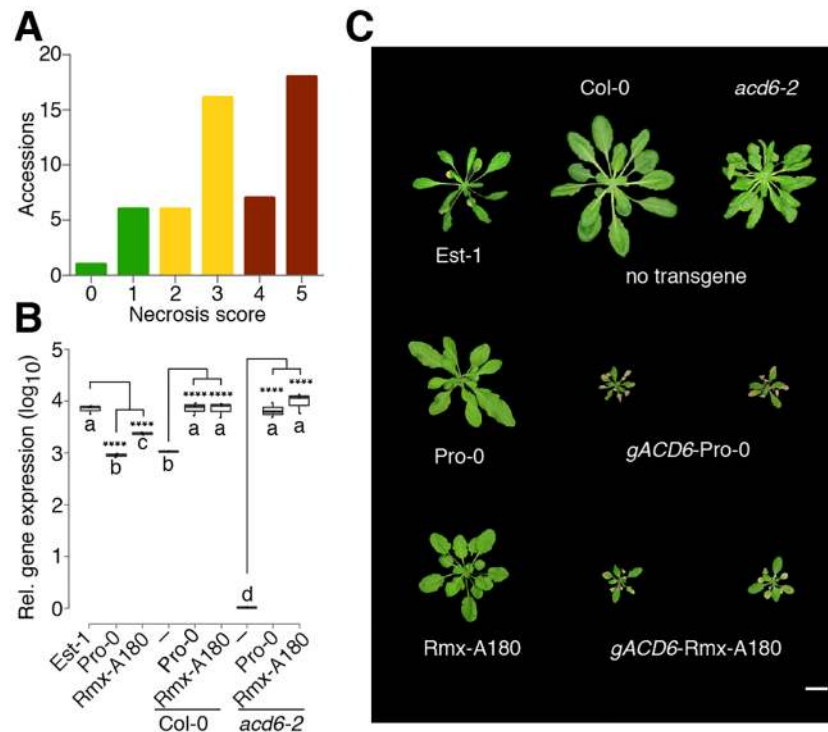
Fig 1. Genetic background dependence of *ACD6*-Est effect. (A) Variation of necrosis in 54 natural accessions (n = 6 each) with *ACD6*-Est alleles. Broad-sense heritability H^2 is 0.89. (B) Accumulation of *ACD6* mRNA in various genetic backgrounds (n = 3), as measured by qRT-PCR. Asterisks indicate significant differences in pairwise Student's t-tests ($p < 0.0001$; Holm adjusted). Letters indicate significantly different groups ($p < 0.0001$; post hoc Tukey's HSD). (C) Representative non-transgenic and *ACD6* transgenic lines at 5 weeks of age in Col-0 and *acd6-2* backgrounds. Est-1, Pro-0 and Rmx-A180 are shown for comparison on the left. Scale bar, 10 mm.

https://doi.org/10.1371/journal.pgen.1007628.g001

individuals suggested more than one locus in all mapping populations (S2 Table). We used RAD-seq [52] followed by QTL mapping to identify causal regions of the genome in these accessions. As expected, we identified multiple significant QTL in all mapping populations (Fig 3A). The QTLs explained 4% to 23% of the observed phenotypic variation, further supporting the quantitative nature of phenotypic suppression of *ACD6*-Est alleles (S3 Table). In most, but not all, cases did the Est-1 allele increase necrosis (S1 Fig).

We decided to focus on the QTL in the center of chromosome 4, near *ACD6*, which explained 18% of phenotypic variance in the Pro-0 x Est-1 cross, because the confidence interval (Chr 4: 7.5–9.7 Mb, LOD = 13.1, p<0.0001) contained a well-studied locus that had been linked to suppression of autoimmunity. Laboratory-induced loss-of-function alleles of this locus, *SNC1*, can fully or partially suppress the phenotypic defects of different autoimmune mutants [53,54]. In addition, *SNC1* gain-of-function alleles reduce plant size, similar to *ACD6* hyperactivity, while down-regulation of *SNC1* homologs increases plant size [19,55]. *SNC1* is located in a complex *NLR* gene cluster, *RECOGNITION OF PERONOSPORA PARASITICA 4/5* (*RPP4/5*), which has alleles that mediate resistance to different strains of the oomycete pathogen *Hyaloperonospora arabidopsidis* [56,57]. *SNC1* and different *RPP4* and *RPP5* alleles are closely related in sequence [19,55,56,58].

To test whether *SNC1* contributes to the suppressed leaf necrosis in Pro-0, and whether *SNC1* can modulate *ACD6* activity, we took a transgene approach. We first introduced a *SNC1*-Pro-0 genomic fragment into Pro-0. This transgene caused autoimmunity, consistent
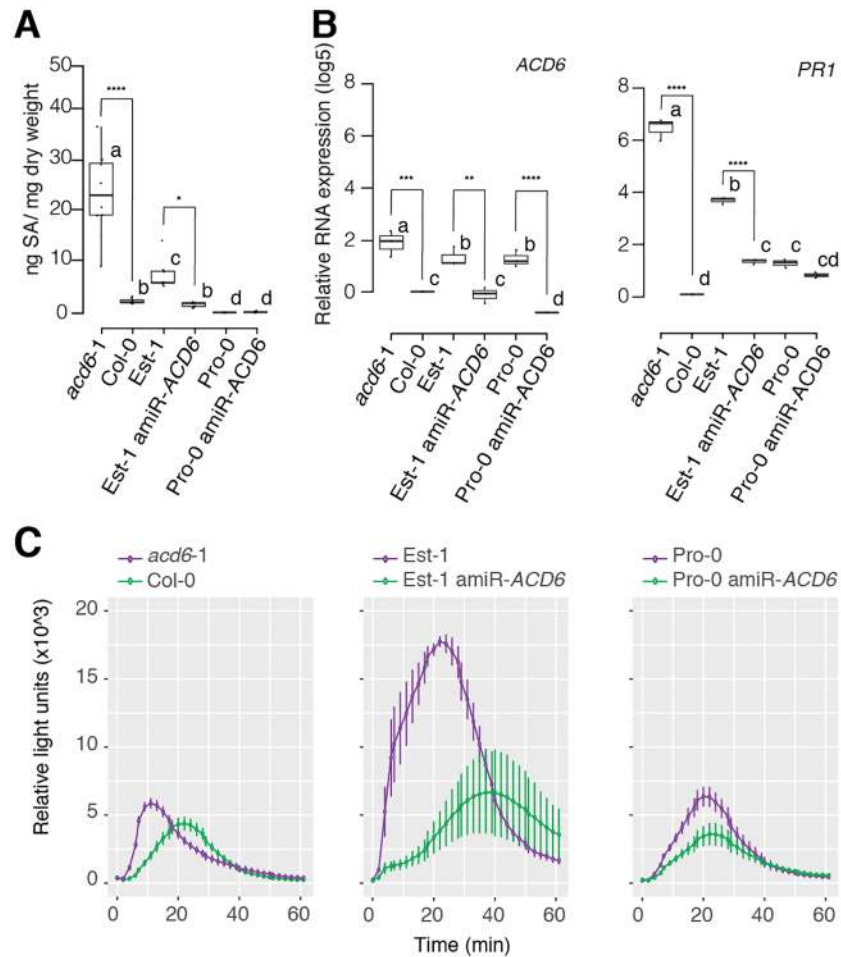
Fig 2. *ACD6*-dependent suppression of salicylic acid accumulation and flg22 responses in Pro-0. (A) SA levels in lines with different *ACD6* alleles, n = 10 per line. Asterisks indicate pairwise Student's t-test results ($p < 0.0001$; Holm adjusted). Letters indicate significantly different groups ($p < 0.0001$; post hoc Tukey's HSD). (B) *ACD6* and *PR1* expression in different T_1 individuals (n = 4), normalized to Col-0. Asterisks indicate significance in pairwise Student's t-tests (*$p < 0.05$, **$p < 0.01$, ***$p < 0.001$, ****$p < 0.0001$; Holm adjusted). Letters indicate significantly different groups ($p < 0.0001$; post hoc Tukey's HSD). (C) H_2O_2 production in response to flg22 (n = 4). Error bars represent standard errors. This experiment was repeated four times with similar results.

https://doi.org/10.1371/journal.pgen.1007628.g002

with additional NLR copies often leading to spontaneous activation of immunity, but the degree of autoimmunity was very modest [59–61]. In contrast, when we introduced a chimeric transgene containing the *SNC1* promoter from Pro-0, but coding sequences from Est-1, into Pro-0, we observed strong necrosis and dwarfism, both in primary transformants and in the T_2 generation (Fig 3B and 3C, S2 Fig). In agreement, Pro-0 plants transformed with the *SNC1*-Est allele were more resistant to infection by *P. syringae* pv. *tomato* strain DC3000 (*Pto* DC3000) than untransformed Pro-0 plants or Pro-0 plants carrying an extra *SNC1*-Pro copy ($p < 0.0001$) (Fig 3D). This suggests that differences in the transcribed portion of *SNC1*, most likely differences between the SNC1-Est and SNC1-Pro proteins, are causal for attenuated effects of *ACD6*-Est alleles. However, since we did not have Near Isogenic Lines (NILs) at our disposal, with which we could directly compare the phenotypic effects of the QTL region with the *SNC1* transgenes, we cannot exclude that the QTL on chromosome 4 includes further genes that contribute to attenuated *ACD6*-Est activity in Pro-0.
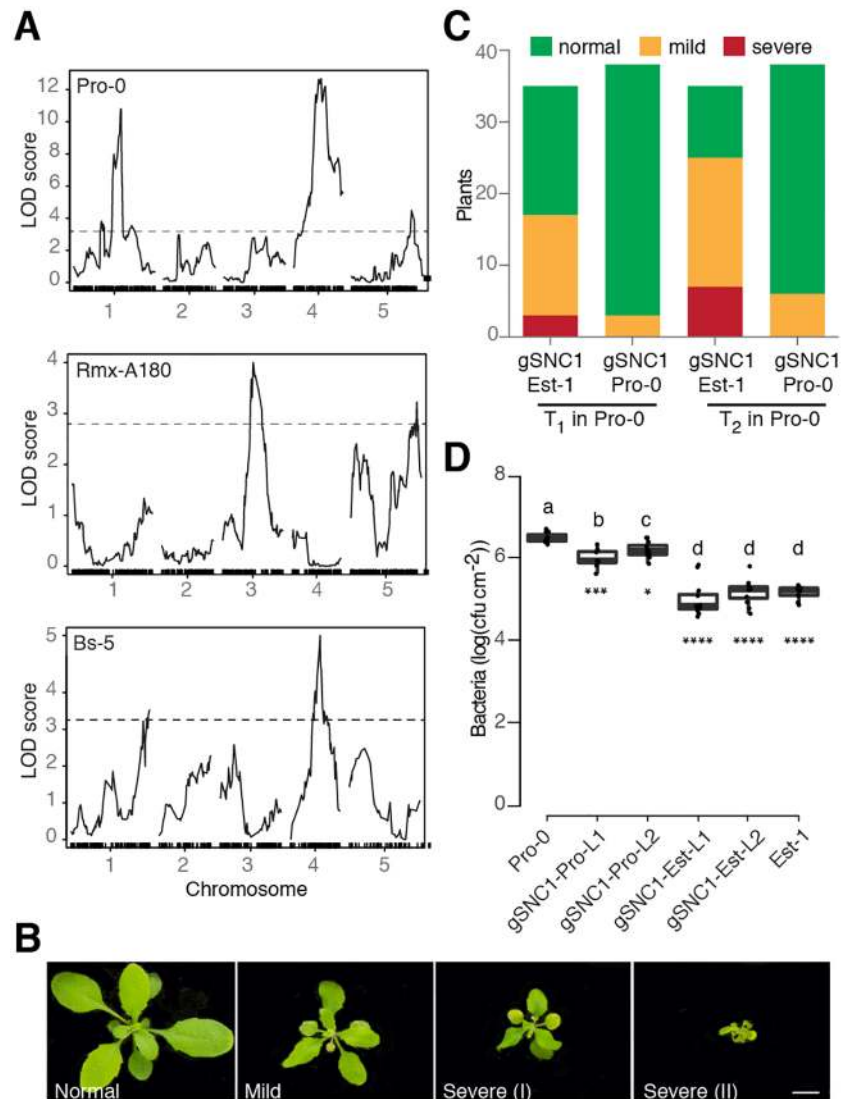
Fig 3. Genetic analysis of *ACD6* modifiers in natural accessions. (A) Necrosis QTL mapping in three F_2 populations. Dashed lines indicate LOD score significance thresholds of $p < 0.05$ (from 1,000 permutations). (B) Representative phenotypes of transformants expressing genomic *SNC1* fragments. Scale bar, 10 mm. (C) Necrosis in transgenic Pro-0 plants. The effects of *SNC1*-Est-1 and *SNC1*-Pro-0 transgenes were significantly different (chi-square test, $p < 0.001$). (D) Growth of Pst DC3000 after infection at $OD_{600} = 0.0001$. Bacterial growth in Pro-0 [*gSNC1*-Pro-0] was significantly different from either Pro-0 [*gSNC1*-Est-1] or nontransgenic Pro-0 on day 3. Asterisks indicate significance in pairwise Student's t-tests against Pro-0 ($^*p < 0.05$, $^{***}p < 0.001$, $^{****} p < 0.0001$; Holm adjusted). Letters indicate significantly different groups ($p < 0.0001$; post hoc Tukey's HSD). L1/L2 designates two independent transgenic lines for both constructs.

https://doi.org/10.1371/journal.pgen.1007628.g003

Correlation of a common *SNC1* structural variant with attenuation of *ACD6* activity

To gauge whether attenuation of *ACD6*-Est activity by variant *SNC1* alleles is likely to be common, we wanted to assess the population frequency of different *SNC1* alleles. We compared the *SNC1* alleles from Est-1 and Pro-0 with *RPP4/RPP5/SNC1*-like sequences from a REN-seq dataset of 65 *A. thaliana* accessions [62]. A protein-phylogeny of 142 *RPP4/RPP5/SNC1* homologs indicated that 34 genes, from 29 accessions, form a single clade of *SNC1* orthologs, which

are predicted to encode highly similar Toll-Interleukin-1 receptor (TIR) domains. Five accessions, Ws-2, Liri-1, Marce-1, DraIV 6–22 and MNF-Che-2, have two *SNC1* homologs each (Fig 4A, S3 Fig, S5 Table). The most noticeable sequence differences among SNC1 proteins affect the NL linker between the nucleotide binding (NB) and leucine-rich repeat (LRR) domains [19]. The NL linker (amino acids 544–671 in SNC1-Col-0) is duplicated in 15 of the 34 SNC1 proteins (Fig 4A and 4B, S3 and S4 Figs). A *SNC1* allele that differs functionally from the Col-0 reference allele has been identified in Ws-2, *SNW* [59]. The *SNC1* homolog that we found in addition to *SNW* in Ws-2 (Ws-2-T078) has a duplicated linker and is highly similar to the Pro-0 variant (Fig 4B, S5 Fig). Similarly, the MNF-Che-2 and DraIV 6–22 accessions have two *SNC1* genes, one each encoding a single and a duplicated linker (Fig 4B). Overall, our analysis revealed a complex history of *SNC1* diversification within and between accessions.

To address whether SNC1 linker variation is associated with suppression of *ACD6* activity across accessions, we determined the *ACD6* allele type in all 15 accessions with the duplicated SNC1 linker. Three accessions, Ty-1, Ct-1 and MNF-Che-2, had *ACD6*-Est alleles (S6 Fig), but only MNF-Che-2 had symptoms of necrosis. This is in agreement with our hypothesis that *SNC1-Pro* allele can function as genetic suppressors of *ACD6* hyperactivity (Fig 4C). That *ACD6*-Est induced necrosis was not suppressed in MNF-Che-2 may be due to the additional *SNC1* homolog without a duplicated linker in this accession (Fig 4C).

Experimental evidence for SNC1 NL linker affecting *ACD6* activity

A gain-of-function allele of *SNC1* induced by EMS mutagenesis, *snc1*-1, has a single amino acid substitution in the NL linker domain, pointing to the functional importance of the NL linker [19]. Since the NL linkers of SNC1 from Pro-0 and Est-1 differ notably, we suspected that they might be responsible for differential *ACD6*-Est effects in different backgrounds. To test this hypothesis, we introduced three different *SNC1* constructs into Col-0: a genomic *SNC1*-Pro fragment, a genomic *SNC1*-Est fragment, and a chimeric *SNC1*-Pro fragment with the dNL linker of Pro-0 replaced with the sNL linker from Est-1. Sixteen of 53 *SNC1*-Est T_1 transgenic plants had a severe autoimmune phenotype (Fig 5A). However, none of 70 *SNC1-Pro* T_1 transgenic plants showed severe, and only 10% showed mild phenotypes. The ability of *SNC1-Pro* in triggering leaf necrosis was fully restored when introducing the SNC1-Est linker in an otherwise Pro-0 protein (SNC1-Pro-NL-Est) (Fig 5A).

To further assess the contribution of the NL linker on SNC1-induced cell-death signaling, we transiently expressed both SNC1-Est and SNC1-Pro in *N. benthamiana* and monitored chlorosis indicative of cell death 7 days after infiltration. Expression of SNC1-Pro resulted in a much weaker cell death and significantly less ion leakage than either SNC1-Est or SNC1-Pro-NL-Est (Fig 5B, S7 Fig). Taken together, we conclude that polymorphisms in the NL linker region explain functional differences between SNC1-Est and SNC1-Pro.

Discussion

The naturally hyperactive *ACD6*-Est allele in *A. thaliana* can induce an autoimmune syndrome associated with necrosis and reduced growth in many, but not all, accessions with this allele [36]. We have shown that variation in the effects of *ACD6*-Est alleles does not map to the *ACD6* locus itself, but rather is caused by extragenic modifiers of the *ACD6*-Est phenotype. Notably, alleles at several different loci can have such an effect, including a common allele at the NLR locus *SNC1*.

Genetic mapping experiments with three different accessions carrying an *ACD6*-Est allele identified a minimum of six genomic regions that can modulate *ACD6*-Est effects. The identified QTL only explain a minority of observed phenotypic variation, suggesting that several
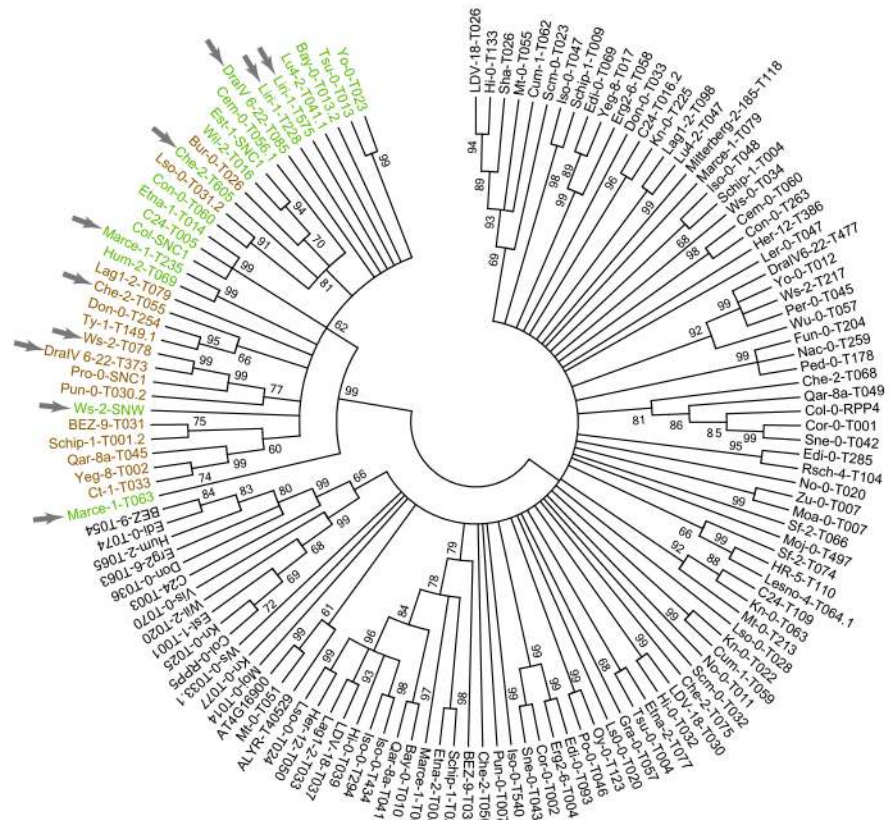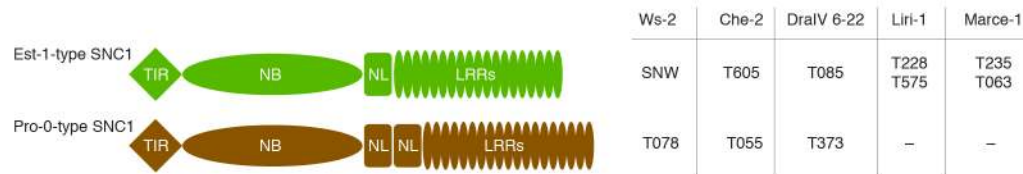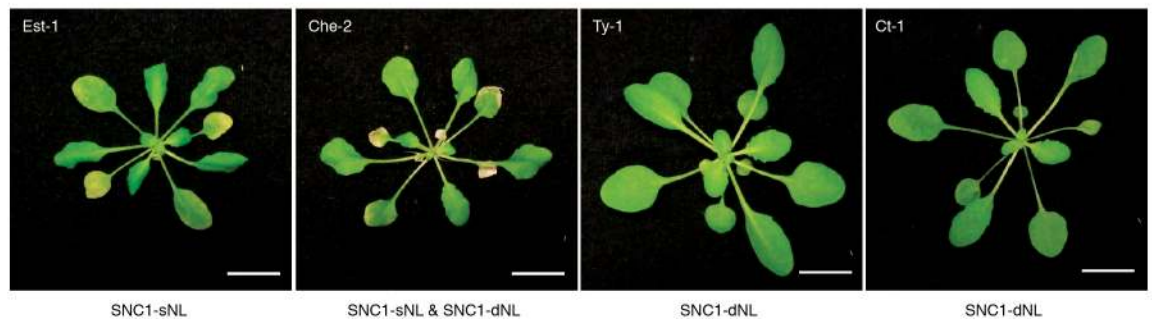
Fig 4. Correlation between *SNC1* alleles and *ACD6*-Est-1 effects in natural accessions. (A) Phylogeny of 136 RPP4/5 and SNC1 proteins from 65 accessions. Bootstrap values over 60% are indicated. The SNC1 clade is highlighted in color, with single NL linker (SNC1-sNL) genes green and duplicated NL linker (SNC1-dNL) genes brown. Arrows highlight five accessions with two *SNC1* homologs. (B) Diagrams of SNC1 proteins with single and duplicated NL linkers. Gene IDs for five accessions with two *SNC1* homologs on the right. (C) Accessions with *ACD6*-Est-like alleles; SNC1 types indicated below. Scale bar, 10 mm.
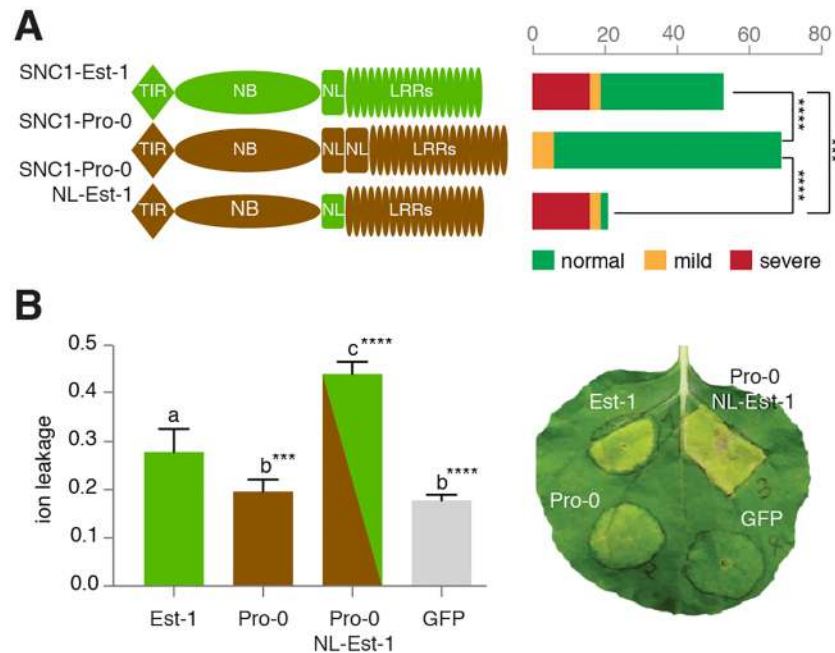
Fig 5. Contribution of NL linker variation to SNC1 activity. (A) Distribution of necrosis in Col-0 T_1 transformants expressing *gSNC1*-Pro-0 with different NL linkers. Asterisks indicate pairwise chi-square test results (*** $p < 0.001$, **** $p < 0.0001$; Holm adjusted). (B) Left, ion leakage, an indicator of cell death, in *N. benthamiana* leaves transiently transformed with different *gSNC1* transgenes 4 d after *Agrobacterium* infiltration. Asterisks indicate significance in pairwise Student's t-tests against Est-1 (*** $p < 0.001$, **** $p < 0.0001$; Holm adjusted). Letters indicate significantly different groups ($p < 0.0001$; post hoc Tukey's HSD). The leaf samples were collected from six independent plants. Right, image of a representative 7-day old leaf after infiltration.

https://doi.org/10.1371/journal.pgen.1007628.g005

additional minor-effect loci contribute to modulation of *ACD6* activity. An attractive hypothesis is that suppressors of *ACD6*-Est-like activity have arisen as a consequence of excessive deleterious effects of *ACD6*-Est and perhaps hyperimmunity alleles at other loci. Alternatively, the *ACD6*-Est allele itself may first have evolved on a background that masked its effects. We found that about a quarter of *A. thaliana* accessions share the *SNC1* allele with a duplicated NL linker, which can attenuate *ACD6*-Est effects. The fraction of accessions with an *ACD6*-Est allele among those with this *SNC1* allele is similar to the frequency of *ACD6*-Est alleles in the global *A. thaliana* population. While there is no obvious indication for linkage between specific *SNC1* and *ACD6* alleles, the numbers examined so far are very small, and the situation could be different in local *A. thaliana* populations. Another explanation for why we did not see an enrichment of specific *SNC1* alleles among *ACD6*-Est carriers might be that other modifiers are more important in natural populations.

It has been argued that tandem duplication of NLR genes within clusters can provide an effective mechanism to acquire novel NLR specificities without sacrificing old ones [63]. *SNC1* features both relevant structural and copy number variation, and functionally distinct variants can occur in the same genome, offering an opportunity to test such hypotheses about NLR evolution. Since *SNC1* has a dosage effect on plant innate immunity [59], it will be interesting to ask whether there are situations in which it is advantageous to have two functionally different *SNC1* copies, as we have seen in MNF-Che-2, Ws-2 and DraIV 6–22.

Mutations in other NLRs can either trigger autoimmunity [19,21–26,64–69] or suppress autoimmunity in various mutants with a range of biochemical defects [67,70–77]. As for *SNC1* itself, the lethality of *bon1* (*bonzai1*) *bon3* double mutants is caused by inappropriate activation

of at least five NLRs, including *SNC1* [77]. Some of the other QTL regions that modify *ACD6*-Est effects include NLR genes as well (S8 Fig), and it will be interesting to learn whether the situation for *ACD6*-Est is similar as for *bon1 bon3* mutants, and whether *ACD6*-Est activity can be attenuated by alleles at NLR loci other than *SNC1*.

In summary, our genetic analyses of accessions with a hyperactive *ACD6* allele have shown that natural *A. thaliana* populations frequently harbor extragenic modulators of *ACD6* activity, underscoring the importance of epistatic interactions for natural phenotypes [29,78–83]. In addition, our work has revealed a new connection between *ACD6*, which has before been primarily linked to PAMP recognition and PTI [34,35,84], and NLR proteins, which are central to ETI. There is already genetic evidence for cell death triggered by PAMP receptor complexes being suppressed by the NLR SNC1 [59,85]. An arbitrary selection of evidence for the distinction between PTI and ETI being fluid [46] includes the overlap in the signaling network downstream of AvrRpt2-triggered ETI and the network activated by the well-known PAMP flg22 [86], or MAPK3 and MAPK6 as widely shared downstream signaling components for both PTI and ETI [86–88]. Together, our findings illustrate the potential of studies of naturally occurring autoimmunity in either *A. thaliana* inbred strains or hybrids [89] to contribute to our understanding of the immune system in healthy and diseased plants.

Methods

Plant material and growth conditions

Seeds of *Arabidopsis thaliana* accessions (S1 and S5 Tables) were from stocks available in the lab. Seeds were germinated and cultivated in growth rooms at a constant temperature of 23˚C (temperature variability about ± 0.1˚C), air humidity of 65% and long days (LD, 16 hr day length) or short days (SD, 8 hr day length), with light (125 to 175 μmol m^{-2} s^{-1}) provided by a 1:1 mixture of Cool White and Gro-Lux Wide Spectrum fluorescent lights (Luxline plus F36W/840, Sylvania, Erlangen, Germany). Leaf necrosis was scored in SD at 23˚C.

qRT-PCR

RNA was extracted from three biological replicates (4- to 5-week-old entire rosettes) using TRIzol Reagent (Thermo Scientific, Waltham, MA) and treated with DNase I (Thermo Scientific, Waltham, MA, USA). 2 μg total RNA was used as a template for reverse transcription (M-MLV reverse transcriptase kit; Thermo Scientific, Waltham, MA, USA). Quantitative real-time PCR reactions were performed using Maxima SYBR Green Master Mix (Thermo Scientific, Waltham, MA, USA) according to the manufacturer's directions on a CFX384 real time instrument (Bio-Rad, Hercules, CA). Transcript abundance was normalized to the *TUBULIN BETA CHAIN 2* (At5g62690) transcript. Relative expression compared to the control (usually Col-0) was quantified based on [90]. Primers used for qRT-PCR are listed in S7 Table.

H$_2$O$_2$ assay

Leaf discs (5 mm diameter) were punched from 5-week-old 23˚C SD-grown plants and immediately floated with the adaxial side up in individual wells of a 96-well plate (Greiner Bio-One, Frickenhausen, Germany) containing 200 μL of water. They were incubated overnight (12–16 hr) covered with a transparent lid, to recover. The water was replaced with the elicitation solution containing 10 μM Luminol (Sigma-Aldrich, MO), 10 μg mL^{-1} horseradish peroxidase and 100 nM flg22 (QRLSTGSRINSAKDDAAGLQIA, >85% purity; EZBiolab, Westfield, IN [91]). H$_2$O$_2$ production was monitored by luminescence immediately after the elicitation solution was added, for at least 90 minutes (Tecan Infinite PRO multimode reader, Tecan, Männedorf,

Switzerland). Controls were mock treated with the same solution without flg22. Each genotype was assayed at least three independent times, with leaves coming from 4 biological replicates each time.

Salicylic acid (SA) quantification

Each sample consisted of 10 (±1) mg freeze-dried, ground plant material of 4-week-old rosettes, with 8 biological replicates per genotype, of plants that had been grown in random-ized complete block design at 23˚C SD. SA was extracted twice with 400 µl 20% methanol (LCMS-grade) / 0.1% hydrofluoroalkane by 5 min ultrasonic extraction, followed by 20 min incubation on ice, and removal of solids by centrifugation for 10 min at 13,500 g. 320 µl super-natant were removed after each extraction step and combined in a new vial. A third extraction step with 400 µl of 100% methanol (conditions see above) was performed and the supernatant was combined with the previous ones. The total volume was split in half before drying in a speed vac. For analysis of the conjugated and free salicylic acid the pellets were redissolved in 30 µl 50% methanol / 0,1% formic acid. Ultra Performance Liquid Chromatography Mass Spectrometry (UPLC-MS) analysis was performed on a Waters Acquity UPLC system coupled to a SYNAPT G2 QTOF mass spectrometer equipped with an ESI-Source (Waters Corpora-tion, Milford, MA) at the University of Tübingen—ZMBP Analytics Laboratory. MassLynx v4.1 was used to control the LCMS system and TargetLynx (Waters Corporation) to perform data integration.

RAD-seq and whole genome genotyping

RAD-seq library preparation using a set of 192 adaptor sequences containing PstI and Mse1 recognition sequences were prepared according to [52,92]. Ninety six or 192 individual sam-ples were pooled per library and sequenced on one Illumina HiSeq 2000 lane (100 bp single-end reads). Raw reads were pre-processed with the SHORE (https://sourceforge.net/projects/shore) pipeline. Default parameters were used for de-multiplexing, read trimming and map-ping. The BWA [93] option, also with default parameters, was used to map the reads to the TAIR9 Col-0 reference genome. The consensus sequences were computed, which were used to create a matrix containing the genotypes at specific marker positions for all F_2 individuals (S4 Table). We only considered bi-allelic SNPs that agreed with SNPs from both parents and the F_1 hybrid of a given cross. Scripts are available at https://github.com/mzaidem/ACD6_suppressors_mapping_RADseq_scripts/tree/master.

QTL mapping and analysis

Pro-0 x Est-1, Rmx-A180 x Est-1 and Bs-5 x Est-1 F_2 individuals were phenotyped for late-onset necrosis in a binary manner. QTL mapping and testing for QTL effects and interactions were performed using the R/qtl package [94]. Lod scores were calculated under a single-QTL model using the function "scanone". Lod score significance thresholds were established using 1,000 permutations. Bayesian credible intervals were estimated for individual QTL. The stan-dard expectation-maximization algorithm was always used as "method." Using the markers closest to the two highest LOD scores, designated as Q1 and Q2, we conducted direct linear modeling. The "Full" model has the equation: y ~ Q1 + Q2 + Q1:Q2, where the additive effect as well as the interaction effect of the selected QTL's are used to calculate the amount of necrotic phenotype variation explained by the model. The "Additive" model (y ~ Q1 + Q2), calculates how much of the necrotic phenotype variation observed is only due to the additive effect of Q1 and Q2. While the "Interaction" model (y ~ Q1:Q2), accounts for how much of the necrotic phenotype variation observed is due to the interaction of Q1 and Q2.

Transgenic lines

ACD6 fragments were amplified from genomic DNA with PCR primers designed based on *ACD6* from Est-1 ([36], S7 Table). The Pro-0 (Rmx-A160) genomic DNA fragment was 9.1 (10.3) kb long, including 2.5 (1.8) kb sequences upstream of the initiation codon and 2.8 (3.2) kb downstream of the stop codon. Restriction enzyme sites of Gibson Assembly (NEB, Ipswich, the USA) were used to generate chimeric constructs [95]. An amiRNA against *ACD6* (TTAATGGTGACTAAAGGCCGT) [36] was used to knock down *ACD6*. All constructs were individually cloned into the Gateway entry vector pCR8/GW/TOPO (Invitrogen) and moved into binary vector pFK206 by LR reaction (Thermo Scientific, Waltham, MA, USA). Constructs in pFK206 were transferred to *Agrobacterium tumefaciens* strain ASE and plants were transformed by floral dipping [96] (S6 Table).

Phylogenetic analysis of RPP4/RPP5/SNC1 protein sequences

SNC1 (AT4G16890), RPP4 (AT4G16860), and RPP5 (AT4G16950) like protein sequences from 63 accessions were extracted from an in-house NLR database of Araport II. These sequences and the single RPP4/5 homolog of *Arabidopsis lyrata* were used as template to query the database with exonerate v2.2.0 allowing a minimal mapping score of 95% [97]. We used MEGA6 [98] to realign these sequences with SNC1-Est-1, SNC1-Pro-0, SNC1-Ws-2 (SNW, GenBank accession AY510018), RPP5-Ler-0 (AF180942) and the RPP4/RPP5/SNC1 homolog At4g16900 from Col-0 (Araport II). One-hundred thirty-six RPP4/5 protein sequences were used to infer phylogenetic relationships with both Neighbor-Joining (NJ) and Maximum likelihood (ML) approaches in MEGA6, either over their entire lengths or only the TIR domain (positions 1–226 in SNC1-Col-0). Node confidence was estimated with 1,000 bootstrap replications. All sequences that we could confidently assign to the SNC1 clade were aligned separately to identify functional polymorphisms. A similar approach was used to generate a phylogenetic tree of ACD6 protein sequences extracted from the in-house NLR database, using ACD6 (AT4G14400) and the adjacent ACD6 homolog AT4G14390 from Araport II as references.

Bacterial infection

Pseudomonas syringae pv tomato strain DC3000 was grown to OD_{600} around 3.0, collected and resuspended in 10 mM $MgCl_2$ at 5×10^5 colony-forming units (cfu)/ml. The bacterial suspension was infiltrated into 4-week-old leaves with a needle-less syringe. Bacterial growth was determined 3 days post inoculation (dpi).

Transient expression in *N. benthamiana* and ion-leakage measurements

Agrobacterium tumefaciens with binary plasmids was grown to OD_{600} of 1.6, and incubated in induction medium (10 mM MES pH 5.6, 10 mM $MgCl_2$ and 150 μM acetosyringone) for three hours. Cell suspensions were normalized to OD_{600} of 0.8 for co-infiltration into the abaxial side of leaves of *N. benthamiana* leaves that had been grown under SD at 23°C. Images were taken 7 days after infiltration. Conductivity assays to measure ion leakage were performed according to [58]. Six independent leaves were infiltrated with *A. tumefaciens* with binary constructs encompassing different *SNC1* alleles and two discs (0.6 mm diameter) were harvested per leaf 5 days after infiltration. The fresh leaves were briefly rinsed with ddH_2O and placed in a tube with 8 ml ddH_2O. Samples were gently shaken for 24 hr before measuring ion content (C1) using an Orion Conductivity (Thermo Scientific, Waltham, MA, USA) instrument. Total ion content (C2) was determined from leaf samples that had been boiled for 15 min. C1/C2

ratios were calculated as indicators of ion leakage. *Nicotiana benthamiana* leaves expressing GFP only were used as control. Statistic differences were calculated by one-way-ANOVA.

Supporting information

S1 Fig. Allele effects for markers closest to the highest LOD score for two significant necrosis QTL in each of the F_2 populations.
(TIF)

S2 Fig. *SNC1* and *PR1* expression in Pro-0 T_2 transformants with mild necrosis, as measured by qRT-PCR.
(TIF)

S3 Fig. Alignment of 34 SNC1 protein sequences from 29 accessions. Gray indicates structural variants including small and large deletions.
(TIF)

S4 Fig. Alignment of duplicated NL linkers from SNC1-Pro-0, with SNC1-Col-0 linker as reference.
(TIF)

S5 Fig. Alignment of SNC1-Pro-0 and T078, a second SNC1 homolog in addition to SNW, which had been previously identified[59] in Ws-2.
(TIF)

S6 Fig. Phylogeny of ACD6 proteins identified from RenSeq. Bootstrap values over 60% are indicated. Est-1-like clade highlighted in red.
(TIF)

S7 Fig. Expression of SNC1 in infiltrated N. benthamiana leaves, as measured by RT-PCR. Samples were harvested 2 d after infiltration.
(TIF)

S8 Fig. Location of ACD6 modifier QTLs compared with that of NLR genes. QTL intervals are indicated by unfilled triangles.
(TIF)

S1 Table. Variation of necrotic phenotype from natural populations with Est-1 like ACD6 allele.
(XLSX)

S2 Table. Phenotypic segregation of ACD6-dependent necrosis phenotype 40 days after sowing, and goodness-of-fit to 3:1 segregation ratio.
(XLSX)

S3 Table. Summary of phenotypic variance explained by individual QTL with and without interaction.
(XLSX)

S4 Table. Genotypes of three F2 mapping populations from crosses of Est-1 to Pro-0, Rmx-A180, and Bs-5.
(XLSX)

S5 Table. Accessions in phylogenetic tree of RPP4/RPP5/SNC1 and gene names.
(XLSX)

S6 Table. Binary T-DNA constructs.
(XLSX)

S7 Table. Primers used for generating constructs and qRT-PCR.
(XLSX)

Acknowledgments

Author Contributions

Conceptualization: Wangsheng Zhu, Maricris Zaidem, Marco Todesco, Rebecca Schwab, Detlef Weigel.

Data curation: Wangsheng Zhu, Maricris Zaidem, Anna-Lena Van de Weyer, Rafal M. Gutaker, Eunyoung Chae, Sang-Tae Kim, Felix Bemm, Lei Li, Frederik Unger, Marcel Janis Beha, Monika Demar.

Formal analysis: Wangsheng Zhu, Maricris Zaidem.

Funding acquisition: Detlef Weigel.

Investigation: Wangsheng Zhu, Maricris Zaidem, Marco Todesco, Detlef Weigel.

Methodology: Wangsheng Zhu, Maricris Zaidem.

Project administration: Rebecca Schwab, Detlef Weigel.

Supervision: Detlef Weigel.

Validation: Wangsheng Zhu, Maricris Zaidem.

Visualization: Wangsheng Zhu, Maricris Zaidem.

Writing – original draft: Wangsheng Zhu, Maricris Zaidem, Detlef Weigel.

Writing – review & editing: Wangsheng Zhu, Maricris Zaidem, Detlef Weigel.

References

1. Maekawa T, Kufer TA, Schulze-Lefert P. NLR functions in plant and animal immune systems: so far and yet so close. Nat Immunol. 2011; 12: 817–826. https://doi.org/10.1038/ni.2083 PMID: 21852785

2. Huot B, Yao J, Montgomery BL, He SY. Growth–Defense Tradeoffs in Plants: A Balancing Act to Optimize Fitness. Mol Plant. 2014; 7: 1267–1287. https://doi.org/10.1093/mp/ssu049 PMID: 24777989

3. Ning Y, Liu W, Wang G-L. Balancing Immunity and Yield in Crop Plants. Trends Plant Sci. 2017; https://doi.org/10.1016/j.tplants.2017.09.010 PMID: 29037452

4. Brown JKM. Yield penalties of disease resistance in crops. Curr Opin Plant Biol. 2002; 5: 339–344. PMID: 12179968

5. Heil M, Baldwin IT. Fitness costs of induced resistance: emerging experimental support for a slippery concept. Trends Plant Sci. 2002; 7: 61–67. PMID: 11832276

6. Burdon JJ, Thrall PH. The fitness costs to plants of resistance to pathogens. Genome Biol. 2003; 4: 227. https://doi.org/10.1186/gb-2003-4-9-227 PMID: 12952527

7. Ellis JG, Lagudah ES, Spielmeyer W, Dodds PN. The past, present and future of breeding rust resistant wheat. Front Plant Sci. 2014; 5: 641. https://doi.org/10.3389/fpls.2014.00641 PMID: 25505474

8. Tellier A, Brown JKM. Spatial heterogeneity, frequency-dependent selection and polymorphism in host-parasite interactions. BMC Evol Biol. 2011; 11: 319. https://doi.org/10.1186/1471-2148-11-319 PMID: 22044632

9. Kroymann J, Mitchell-Olds T. Epistasis and balanced polymorphism influencing complex trait variation. Nature. 2005; 435: 95–98. https://doi.org/10.1038/nature03480 PMID: 15875023

10. Tian D, Araki H, Stahl E, Bergelson J, Kreitman M. Signature of balancing selection in Arabidopsis. Proc Natl Acad Sci U S A. 2002; 99: 11525–11530. https://doi.org/10.1073/pnas.172203599 PMID: 12172007

11. Tian D, Traw MB, Chen JQ, Kreitman M, Bergelson J. Fitness costs of R-gene-mediated resistance in Arabidopsis thaliana. Nature. 2003; 423: 74–77. https://doi.org/10.1038/nature01588 PMID: 12721627

12. Yamamoto E, Takashi T, Morinaka Y, Lin S, Wu J, Matsumoto T, et al. Gain of deleterious function causes an autoimmune response and Bateson-Dobzhansky-Muller incompatibility in rice. Mol Genet Genomics. 2010; 283: 305–315. https://doi.org/10.1007/s00438-010-0514-y PMID: 20140455

13. Karasov TL, Kniskern JM, Gao L, DeYoung BJ, Ding J, Dubiella U, et al. The long-term maintenance of a resistance polymorphism through diffuse interactions. Nature. 2014; 512: 436–440. https://doi.org/10.1038/nature13439 PMID: 25043057

14. Sicard A, Kappel C, Josephs EB, Lee YW, Marona C, Stinchcombe JR, et al. Divergent sorting of a balanced ancestral polymorphism underlies the establishment of gene-flow barriers in *Capsella*. Nat Commun. Nature Publishing Group; 2015; 6: ncomms8960.

15. Periyannan S, Moore J, Ayliffe M, Bansal U, Wang X, Huang L, et al. The gene Sr33, an ortholog of barley Mla genes, encodes resistance to wheat stem rust race Ug99. Science. 2013; 341: 786–788. https://doi.org/10.1126/science.1239028 PMID: 23811228

16. Jones JDG, Vance RE, Dangl JL. Intracellular innate immune surveillance devices in plants and animals. Science. 2016; 354. https://doi.org/10.1126/science.aaf6395 PMID: 27934708

17. Zhang X, Dodds PN, Bernoux M. What Do We Know About NOD-Like Receptors In Plant Immunity? Annu Rev Phytopathol. 2017; https://doi.org/10.1146/annurev-phyto-080516-035250 PMID: 28637398

18. Baggs E, Dagdas G, Krasileva KV. NLR diversity, helpers and integrated domains: making sense of the NLR IDentity. Curr Opin Plant Biol. 2017/8; 38: 59–67. https://doi.org/10.1016/j.pbi.2017.04.012 PMID: 28494248

19. Zhang Y, Goritschnig S, Dong X, Li X. A gain-of-function mutation in a plant disease resistance gene leads to constitutive activation of downstream signal transduction pathways in suppressor of npr1-1, constitutive 1. Plant Cell. 2003; 15: 2636–2646. https://doi.org/10.1105/tpc.015842 PMID: 14576290

20. Gao Z, Gao Z, Chung E-H, Eitas TK, Dangl JL. Plant intracellular innate immune receptor Resistance to Pseudomonas syringae pv. maculicola 1 (RPM1) is activated at, and functions on, the plasma membrane. Proc Natl Acad Sci U S A. 2011; 108: 7619–7624. https://doi.org/10.1073/pnas.1104410108 PMID: 21490299

21. Shirano Y, Kachroo P, Shah J, Klessig DF. A gain-of-function mutation in an Arabidopsis Toll Interleukin1 receptor-nucleotide binding site-leucine-rich repeat type R gene triggers defense responses and results in enhanced disease resistance. Plant Cell. 2002; 14: 3149–3162. https://doi.org/10.1105/tpc.005348 PMID: 12468733

22. Noutoshi Y, Ito T, Seki M, Nakashita H, Yoshida S, Marco Y, et al. A single amino acid insertion in the WRKY domain of the Arabidopsis TIR-NBS-LRR-WRKY-type disease resistance protein SLH1 (sensitive to low humidity 1) causes activation of defense responses and hypersensitive cell death. Plant J. 2005; 43: 873–888. https://doi.org/10.1111/j.1365-313X.2005.02500.x PMID: 16146526

23. Yang H, Shi Y, Liu J, Guo L, Zhang X, Yang S. A mutant CHS3 protein with TIR-NB-LRR-LIM domains modulates growth, cell death and freezing tolerance in a temperature-dependent manner in Arabidopsis. Plant J. 2010; 63: 283–296. https://doi.org/10.1111/j.1365-313X.2010.04241.x PMID: 20444230

24. Huang X, Li J, Bao F, Zhang X, Yang S. A gain-of-function mutation in the Arabidopsis disease resistance gene RPP4 confers sensitivity to low temperature. Plant Physiol. 2010; 154: 796–809. https://doi.org/10.1104/pp.110.157610 PMID: 20699401

25. Igari K, Endo S, Hibara K-I, Aida M, Sakakibara H, Kawasaki T, et al. Constitutive activation of a CC-NB-LRR protein alters morphogenesis through the cytokinin pathway in Arabidopsis. Plant J. 2008; 55: 14–27. https://doi.org/10.1111/j.1365-313X.2008.03466.x PMID: 18315541

26. Bi D, Johnson KCM, Zhu Z, Huang Y, Chen F, Zhang Y, et al. Mutations in an Atypical TIR-NB-LRR-LIM Resistance Protein Confer Autoimmunity. Front Plant Sci. 2011; 2: 71. https://doi.org/10.3389/fpls.2011.00071 PMID: 22639607

27. Shah SJA, Hussain S, Ahmad M, Farhatullah, Ali I, Ibrahim M. Using leaf tip necrosis as a phenotypic marker to predict the presence of durable rust resistance gene pair Lr34/Yr18 in wheat. J Gen Plant Pathol. 2011; 77: 174–177. https://doi.org/10.1007/s10327-011-0301-6

28. Corwin JA, Kliebenstein DJ. Quantitative Resistance: More Than Just Perception of a Pathogen. Plant Cell. 2017; 29: 655–665. https://doi.org/10.1105/tpc.16.00915 PMID: 28302676

29. Iakovidis M, Teixeira PJPL, Exposito-Alonso M, Cowper MG, Law TF, Liu Q, et al. Effector-Triggered Immune Response in Arabidopsis thaliana Is a Quantitative Trait. Genetics. 2016; 204: 337–353. https://doi.org/10.1534/genetics.116.190678 PMID: 27412712

30. Yang Q, Balint-Kurti P, Xu M. Quantitative Disease Resistance: Dissection and Adoption in Maize. Mol Plant. 2017; 10: 402–413. https://doi.org/10.1016/j.molp.2017.02.004 PMID: 28254471

31. Kou Y, Wang S. Broad-spectrum and durability: understanding of quantitative disease resistance. Curr Opin Plant Biol. 2010; 13: 181–185. https://doi.org/10.1016/j.pbi.2009.12.010 PMID: 20097118

32. Rate DN, Cuenca JV, Bowman GR, Guttman DS, Greenberg JT. The gain-of-function Arabidopsis acd6 mutant reveals novel regulation and function of the salicylic acid signaling pathway in controlling cell death, defenses, and cell growth. Plant Cell. 1999; 11: 1695–1708. PMID: 10488236

33. Lu H, Rate DN, Song JT, Greenberg JT. ACD6, a novel ankyrin protein, is a regulator and an effector of salicylic acid signaling in the Arabidopsis defense response. Plant Cell. 2003; 15: 2408–2420. https://doi.org/10.1105/tpc.015412 PMID: 14507999

34. Tateda C, Zhang Z, Shrestha J, Jelenska J, Chinchilla D, Greenberg JT. Salicylic acid regulates Arabidopsis microbial pattern receptor kinase levels and signaling. Plant Cell. 2014; 26: 4171–4187. https://doi.org/10.1105/tpc.114.131938 PMID: 25315322

35. Zhang Z, Tateda C, Jiang S-C, Shrestha J, Jelenska J, Speed DJ, et al. A suite of receptor-like kinases and a putative mechano-sensitive channel are involved in autoimmunity and plasma membrane-based defenses in Arabidopsis. Mol Plant Microbe Interact. 2017; https://doi.org/10.1094/MPMI-09-16-0184-R PMID: 28051349

36. Todesco M, Balasubramanian S, Hu TT, Traw MB, Horton M, Epple P, et al. Natural allelic variation underlying a major fitness trade-off in Arabidopsis thaliana. Nature. 2010; 465: 632–636. https://doi.org/10.1038/nature09083 PMID: 20520716

37. Świadek M, Proost S, Sieh D, Yu J, Todesco M, Jorzig C, et al. Novel allelic variants in ACD6 cause hybrid necrosis in local collection of Arabidopsis thaliana. New Phytol. 2016; https://doi.org/10.1111/nph.14155 PMID: 27588563

38. Todesco M, Kim S-T, Chae E, Bomblies K, Zaidem M, Smith LM, et al. Activation of the Arabidopsis thaliana immune system by combinations of common ACD6 alleles. PLoS Genet. 2014; 10: e1004459. https://doi.org/10.1371/journal.pgen.1004459 PMID: 25010663

39. Fusari CM, Kooke R, Lauxmann MA, Annunziata MG, Encke B, Hoehne M, et al. Genome-wide Association Mapping Reveals that Specific and Pleiotropic Regulatory Mechanisms Fine-tune Central Metabolism and Growth in Arabidopsis. Plant Cell. American Society of Plant Biologists; 2017; https://doi.org/10.1105/tpc.17.00232 PMID: 28954812

40. Flood PJ. Natural genetic variation in Arabidopsis thaliana photosynthesis. http://edepot.wur.nl/361162

41. Kerwin R, Feusier J, Corwin J, Rubin M, Lin C, Muok A, et al. Natural genetic variation in Arabidopsis thaliana defense metabolism genes modulates field fitness. Elife. 2015; 4. https://doi.org/10.7554/eLife.05604 PMID: 25867014

42. Weinhold A, Karimi Dorcheh E, Li R, Rameshkumar N, Baldwin IT. Antimicrobial peptide expression in a wild tobacco plant reveals the limits of host-microbe-manipulations in the field. Elife. 2018; 7. https://doi.org/10.7554/eLife.28715 PMID: 29661271

43. Malmberg RL, Held S, Waits A, Mauricio R. Epistasis for fitness-related quantitative traits in Arabidopsis thaliana grown in the field and in the greenhouse. Genetics. 2005; 171: 2013–2027. https://doi.org/10.1534/genetics.105.046078 PMID: 16157670

44. Corwin JA, Copeland D, Feusier J, Subedy A, Eshbaugh R, Palmer C, et al. The Quantitative Basis of the Arabidopsis Innate Immune System to Endemic Pathogens Depends on Pathogen Genetics. PLoS Genet. 2016; 12: e1005789. https://doi.org/10.1371/journal.pgen.1005789 PMID: 26866607

45. Zhang N, Lariviere A, Tonsor SJ, Traw MB. Constitutive camalexin production and environmental stress response variation in Arabidopsis populations from the Iberian Peninsula. Plant Sci. 2014; 225: 77–85. https://doi.org/10.1016/j.plantsci.2014.05.020 PMID: 25017162

46. Thomma BP, Nürnberger T, Joosten MH. Of PAMPs and effectors: the blurred PTI-ETI dichotomy. Plant Cell. 2011; 23: 4–15. https://doi.org/10.1105/tpc.110.082602 PMID: 21278123

47. Ondov BD, Treangen TJ, Melsted P, Mallonee AB, Bergman NH, Koren S, et al. Mash: fast genome and metagenome distance estimation using MinHash. Genome Biol. 2016; 17: 132. https://doi.org/10.1186/s13059-016-0997-x PMID: 27323842

48. 1001 Genomes Consortium. 1,135 Genomes reveal the global pattern of polymorphism in Arabidopsis thaliana. Cell. 2016; 166: 481–491. https://doi.org/10.1016/j.cell.2016.05.063 PMID: 27293186

49. Spoel SH, Dong X. How do plants achieve immunity? Defence without specialized immune cells. Nat Rev Immunol. 2012; 12: 89–100. https://doi.org/10.1038/nri3141 PMID: 22273771

50. Schwab R, Ossowski S, Riester M, Warthmann N, Weigel D. Highly specific gene silencing by artificial microRNAs in Arabidopsis. Plant Cell. 2006; 18: 1121–1133. https://doi.org/10.1105/tpc.105.039834 PMID: 16531494

51. Boller T, Felix G. A renaissance of elicitors: perception of microbe-associated molecular patterns and danger signals by pattern-recognition receptors. Annu Rev Plant Biol. 2009; 60: 379–406. https://doi.org/10.1146/annurev.arplant.57.032905.105346 PMID: 19400727

52. Rowan BA, Seymour DK, Chae E, Lundberg DS, Weigel D. Methods for Genotyping-by-Sequencing. Methods Mol Biol. 2017; 1492: 221–242. https://doi.org/10.1007/978-1-4939-6442-0_16 PMID: 27822868

53. Li Y, Li S, Bi D, Cheng YT, Li X, Zhang Y. SRFR1 negatively regulates plant NB-LRR resistance protein accumulation to prevent autoimmunity. PLoS Pathog. 2010; 6: e1001111. https://doi.org/10.1371/journal.ppat.1001111 PMID: 20862316

54. Gou M, Hua J. Complex regulation of an R gene SNC1 revealed by auto-immune mutants. Plant Signal Behav. 2012; 7: 213–216. https://doi.org/10.4161/psb.18884 PMID: 22415045

55. Yi H, Richards EJ. A cluster of disease resistance genes in Arabidopsis is coordinately regulated by transcriptional activation and RNA silencing. Plant Cell. 2007; 19: 2929–2939. https://doi.org/10.1105/tpc.107.051821 PMID: 17890374

56. van der Biezen EA, Freddie CT, Kahn K, Parker JE, Jones JDG. Arabidopsis RPP4 is a member of the RPP5 multigene family of TIR-NB-LRR genes and confers downy mildew resistance through multiple signalling components. Plant J. 2002; 29: 439–451. PMID: 11846877

57. Parker JE, Coleman MJ, Szabò V, Frost LN, Schmidt R, van der Biezen EA, et al. The Arabidopsis downy mildew resistance gene RPP5 shares similarity to the toll and interleukin-1 receptors with N and L6. Plant Cell. 1997; 9: 879–894. PMID: 9212464

58. Zhang X, Bernoux M, Bentham AR, Newman TE, Ve T, Casey LW, et al. Multiple functional self-association interfaces in plant TIR domains. Proc Natl Acad Sci U S A. 2017; 114: E2046–E2052. https://doi.org/10.1073/pnas.1621248114 PMID: 28159890

59. Yang S, Hua J. A haplotype-specific Resistance gene regulated by BONZAI1 mediates temperature-dependent growth control in Arabidopsis. Plant Cell. 2004; 16: 1060–1071. https://doi.org/10.1105/tpc.020479 PMID: 15031411

60. Stokes TL, Kunkel BN, Richards EJ. Epigenetic variation in Arabidopsis disease resistance. Genes Dev. 2002; 16: 171–182. https://doi.org/10.1101/gad.952102 PMID: 11799061

61. Li X, Kapos P, Zhang Y. NLRs in plants. Curr Opin Immunol. 2015; 32: 114–121. https://doi.org/10.1016/j.coi.2015.01.014 PMID: 25667191

62. Jupe F, Witek K, Verweij W, Sliwka J, Pritchard L, Etherington GJ, et al. Resistance gene enrichment sequencing (RenSeq) enables reannotation of the NB-LRR gene family from sequenced plant genomes and rapid mapping of resistance loci in segregating populations. Plant J. 2013; 76: 530–544. https://doi.org/10.1111/tpj.12307 PMID: 23937694

63. Urbach JM, Ausubel FM. The NBS-LRR architectures of plant R-proteins and metazoan NLRs evolved in independent events. Proc Natl Acad Sci U S A. 2017; https://doi.org/10.1073/pnas.1619730114 PMID: 28096345

64. Bonardi V, Tang S, Stallmann A, Roberts M, Cherkis K, Dangl JL. Expanded functions for a family of plant intracellular immune receptors beyond specific recognition of pathogen effectors. Proc Natl Acad Sci U S A. 2011; 108: 16463–16468. https://doi.org/10.1073/pnas.1113726108 PMID: 21911370

65. Roberts M, Tang S, Stallmann A, Dangl JL, Bonardi V. Genetic requirements for signaling from an auto-active plant NB-LRR intracellular innate immune receptor. PLoS Genet. 2013; 9: e1003465. https://doi.org/10.1371/journal.pgen.1003465 PMID: 23633962

66. Zbierzak AM, Porfirova S, Griebel T, Melzer M, Parker JE, Dörmann P. A TIR-NBS protein encoded by Arabidopsis Chilling Sensitive 1 (CHS1) limits chloroplast damage and cell death at low temperature. Plant J. 2013; 75: 539–552. https://doi.org/10.1111/tpj.12219 PMID: 23617639

67. Atanasov KE, Liu C, Erban A, Kopka J, Parker JE, Alcázar R. NLR mutations suppressing immune hybrid incompatibility and their effects on disease resistance. Plant Physiol. 2018; https://doi.org/10.1104/pp.18.00462 PMID: 29794019

68. Berkey R, Zhang Y, Ma X, King H, Zhang Q, Wang W, et al. Homologues of the RPW8 Resistance Protein Are Localized to the Extrahaustorial Membrane that Is Likely Synthesized De Novo. Plant Physiol. 2017; 173: 600–613. https://doi.org/10.1104/pp.16.01539 PMID: 27856916

69. Tang J, Zhu X, Wang Y, Liu L, Xu B, Li F, et al. Semi-dominant mutations in the CC-NB-LRR-type R gene, NLS1, lead to constitutive activation of defense responses in rice. Plant J. 2011; 66: 996–1007. https://doi.org/10.1111/j.1365-313X.2011.04557.x PMID: 21418352

70. Palma K, Thorgrimsen S, Malinovsky FG, Fiil BK, Nielsen HB, Brodersen P, et al. Autoimmunity in Arabidopsis acd11 is mediated by epigenetic regulation of an immune receptor. PLoS Pathog. 2010; 6: e1001137. https://doi.org/10.1371/journal.ppat.1001137 PMID: 20949080

71. Lolle S, Greeff C, Petersen K, Roux M, Jensen MK, Bressendorff S, et al. Matching NLR Immune Receptors to Autoimmunity in camta3 Mutants Using Antimorphic NLR Alleles. Cell Host Microbe. 2017; 21: 518–529.e4. https://doi.org/10.1016/j.chom.2017.03.005 PMID: 28407487

72. Zhao T, Rui L, Li J, Nishimura MT, Vogel JP, Liu N, et al. A truncated NLR protein, TIR-NBS2, is required for activated defense responses in the exo70B1 mutant. PLoS Genet. 2015; 11: e1004945. https://doi.org/10.1371/journal.pgen.1004945 PMID: 25617755

73. Bao Z, Yang H, Hua J. Perturbation of cell cycle regulation triggers plant immune response via activation of disease resistance genes. Proc Natl Acad Sci U S A. 2013; 110: 2407–2412. https://doi.org/10.1073/pnas.1217024110 PMID: 23345424

74. Zhang Y, Wang Y, Liu J, Ding Y, Wang S, Zhang X, et al. Temperature-dependent autoimmunity mediated by chs1 requires its neighboring TNL gene SOC3. New Phytol. 2017; 213: 1330–1345. https://doi.org/10.1111/nph.14216 PMID: 27699788

75. Stuttmann J, Peine N, Garcia AV, Wagner C, Choudhury SR, Wang Y, et al. Arabidopsis thaliana DM2h (R8) within the Landsberg RPP1-like Resistance Locus Underlies Three Different Cases of EDS1-Conditioned Autoimmunity. PLoS Genet. 2016; 12: e1005990. https://doi.org/10.1371/journal.pgen.1005990 PMID: 27082651

76. Zhang Z, Wu Y, Gao M, Zhang J, Kong Q, Liu Y, et al. Disruption of PAMP-induced MAP kinase cascade by a Pseudomonas syringae effector activates plant immunity mediated by the NB-LRR protein SUMM2. Cell Host Microbe. 2012; 11: 253–263. https://doi.org/10.1016/j.chom.2012.01.015 PMID: 22423965

77. Li Y, Pennington BO, Hua J. Multiple R-like genes are negatively regulated by BON1 and BON3 in arabidopsis. Mol Plant Microbe Interact. 2009; 22: 840–848. https://doi.org/10.1094/MPMI-22-7-0840 PMID: 19522566

78. Xing Z, Tan F, Hua P, Sun L, Xu G, Zhang Q. Characterization of the main effects, epistatic effects and their environmental interactions of QTLs on the genetic basis of yield traits in rice. Theor Appl Genet. 2002; 105: 248–257. https://doi.org/10.1007/s00122-002-0952-y PMID: 12582526

79. Paaby AB, Rockman MV. Cryptic genetic variation: evolution's hidden substrate. Nat Rev Genet. 2014; 15: 247–258. https://doi.org/10.1038/nrg3688 PMID: 24614309

80. Chow CY, Kelsey KJP, Wolfner MF, Clark AG. Candidate genetic modifiers of retinitis pigmentosa identified by exploiting natural variation in Drosophila. Hum Mol Genet. 2016; 25: 651–659. https://doi.org/10.1093/hmg/ddv502 PMID: 26662796

81. Huang W, Richards S, Carbone MA, Zhu D, Anholt RRH, Ayroles JF, et al. Epistasis dominates the genetic architecture of Drosophila quantitative traits. Proc Natl Acad Sci U S A. 2012; 109: 15553–15559. https://doi.org/10.1073/pnas.1213423109 PMID: 22949659

82. Khan AI, Dinh DM, Schneider D, Lenski RE, Cooper TF. Negative epistasis between beneficial mutations in an evolving bacterial population. Science. 2011; 332: 1193–1196. https://doi.org/10.1126/science.1203801 PMID: 21636772

83. Chae E, Bomblies K, Kim S-T, Karelina D, Zaidem M, Ossowski S, et al. Species-wide genetic incompatibility analysis identifies immune genes as hot spots of deleterious epistasis. Cell. 2014; 159: 1341–1351. https://doi.org/10.1016/j.cell.2014.10.049 PMID: 25467443

84. Zhang Z, Shrestha J, Tateda C, Greenberg JT. Salicylic acid signaling controls the maturation and localization of the arabidopsis defense protein ACCELERATED CELL DEATH6. Mol Plant. 2014; 7: 1365–1383. https://doi.org/10.1093/mp/ssu072 PMID: 24923602

85. Bartels S, Anderson JC, González Besteiro MA, Carreri A, Hirt H, Buchala A, et al. MAP kinase phosphatase1 and protein tyrosine phosphatase1 are repressors of salicylic acid synthesis and SNC1-mediated responses in Arabidopsis. Plant Cell. 2009; 21: 2884–2897. https://doi.org/10.1105/tpc.109.067678 PMID: 19789277

86. Tsuda K, Sato M, Stoddard T, Glazebrook J, Katagiri F. Network properties of robust immunity in plants. PLoS Genet. 2009; 5: e1000772. https://doi.org/10.1371/journal.pgen.1000772 PMID: 20011122

87. Underwood W, Zhang S, He SY. The Pseudomonas syringae type III effector tyrosine phosphatase HopAO1 suppresses innate immunity in Arabidopsis thaliana. Plant J. 2007; 52: 658–672. https://doi.org/10.1111/j.1365-313X.2007.03262.x PMID: 17877704

88. Sato M, Tsuda K, Wang L, Coller J, Watanabe Y, Glazebrook J, et al. Network modeling reveals prevalent negative regulatory relationships between signaling sectors in Arabidopsis immune signaling. PLoS Pathog. 2010; 6: e1001011. https://doi.org/10.1371/journal.ppat.1001011 PMID: 20661428

89. Chae E, Tran DTN, Weigel D. Cooperation and Conflict in the Plant Immune System. PLoS Pathog. 2016; 12: e1005452. https://doi.org/10.1371/journal.ppat.1005452 PMID: 26986469

90. Pfaffl MW. A new mathematical model for relative quantification in real-time RT-PCR. Nucleic Acids Res. 2001; 29: e45. PMID: 11328886

91. Felix G, Duran JD, Volko S, Boller T. Plants have a sensitive perception system for the most conserved domain of bacterial flagellin. Plant J. 1999; 18: 265–276. http://doi.org/10.1046/j.1365-313X.1999.00265.x PMID: 10377992

92. Poland JA, Brown PJ, Sorrells ME, Jannink J-L. Development of High-Density Genetic Maps for Barley and Wheat Using a Novel Two-Enzyme Genotyping-by-Sequencing Approach. PLoS One. 2012; 7: e32253. https://doi.org/10.1371/journal.pone.0032253 PMID: 22389690

93. Li H, Durbin R. Fast and accurate short read alignment with Burrows-Wheeler transform. Bioinformatics. 2009; 25: 1754–1760. https://doi.org/10.1093/bioinformatics/btp324 PMID: 19451168

94. Broman KW, Wu H, Sen S, Churchill GA. R/qtl: QTL mapping in experimental crosses. Bioinformatics. 2003; 19: 889–890. PMID: 12724300

95. Gibson DG, Young L, Chuang R-Y, Venter JC, Hutchison CA 3rd, Smith HO. Enzymatic assembly of DNA molecules up to several hundred kilobases. Nat Methods. 2009; 6: 343–345. https://doi.org/10.1038/nmeth.1318 PMID: 19363495

96. Clough SJ, Bent AF. Floral dip: a simplified method for Agrobacterium-mediated transformation of Arabidopsis thaliana. Plant J. 1998; 16: 735–743. PMID: 10069079

97. Slater GSC, Birney E. Automated generation of heuristics for biological sequence comparison. BMC Bioinformatics. 2005; 6: 31. https://doi.org/10.1186/1471-2105-6-31 PMID: 15713233

98. Tamura K, Stecher G, Peterson D, Filipski A, Kumar S. MEGA6: Molecular Evolutionary Genetics Analysis version 6.0. Mol Biol Evol. 2013; 30: 2725–2729. https://doi.org/10.1093/molbev/mst197 PMID: 24132122